Biochimica et Biophysica Acta 1788 (2009) 993–1008

Contents lists available at ScienceDirect

Biochimica et Biophysica Acta

journal homepage: www.elsevier.com/locate/bbamem

Extrusion of transmitter, water and ions generates forces to close fusion pore

M. Tajparast [a], M.I. Glavinović [b,*]

[a] Department of Civil Engineering, McGill University, Montreal, PQ, Canada
[b] Department of Physiology, McGill University, 3655 Sir William Osler Promenade, Montreal, P.Q., Canada H3G 1Y6

ARTICLE INFO

Article history:
Received 23 August 2008
Received in revised form 7 January 2009
Accepted 30 January 2009
Available online 11 February 2009

Keywords:
Fusion pore
Nanofluidic
Transmitter
Pore dynamics
Exocytosis
Poisson–Nernst–Planck
Navier–Stokes
Transport
Porous media
Nano-electromechanical system

ABSTRACT

During exocytosis the fusion pore opens rapidly, then dilates gradually, and may subsequently close completely, but what controls its dynamics is not well understood. In this study we focus our attention on forces acting on the pore wall, and which are generated solely by the passage of transmitter, ions and water through the open fusion pore. The transport through the charged cylindrical nano-size pore is simulated using a coupled system of Poisson–Nernst–Planck and Navier–Stokes equations and the forces that act radially on the wall of the fusion pore are then estimated. Four forces are considered: a) inertial force, b) pressure, c) viscotic force, and d) electrostatic force. The inertial and viscotic forces are small, but the electrostatic force and the pressure are typically significant. High vesicular pressure tends to open the fusion pore, but the pressure induced by the transport of charged particles (glutamate, ions), which is predominant when the pore wall charge density is high tends to close the pore. The electrostatic force, which also depends on the charge density on the pore wall, is weakly repulsive before the pore dilates, but becomes attractive and pronounced as the pore dilates. Given that the vesicular concentration of free transmitter can change rapidly due to the release, or owing to the dissociation from the gel matrix, we evaluated how much and how rapidly a change of the vesicular K^+–glutamate$^-$ concentration affects the concentration of glutamate$^-$ and ions in the pore and how such changes alter the radial force on the wall of the fusion pore. A step-like rise of the vesicular K^+–glutamate$^-$ concentration leads to a chain of events. Pore concentration (and efflux) of both K^+ and glutamate$^-$ rise reaching their new steady-state values in less than 100 ns. Interestingly within a similar time interval the pore concentration of Na^+ also rises, whereas that of Cl^- diminishes, although their extra-cellular concentration does not change. Finally such changes affect also the water movement. Water efflux changes bi-phasically, first increasing before decreasing to a new, but lower steady-state value. Nevertheless, even under such conditions an overall approximate neutrality of the pore is maintained remarkably well, and the electrostatic, but also inertial, viscotic and pressure forces acting on the pore wall remain constant. In conclusion the extrusion of the vesicular content generates forces, primarily the force due to the electro-kinetically induced pressure and electrostatic force (both influenced by the pore radius and even more by the charge density on the pore wall), which tend to close the fusion pore.

1. Introduction

Hormones, transmitters and peptides are released from secretory cells by exocytosis of vesicles (synaptic, large dense-core vesicles and other types of vesicles) or granules. During exocytosis the first aqueous connection that forms between the lumen of a secretory vesicle and the cell exterior is provided by the formation of a fusion pore [1]. Following its opening the fusion pore expands, but this expansion may stop and be reversed, and the pore may close completely [2]. Dynamics of the pore opening and closing may critically influence how rapidly hormones, transmitters or peptides are released into the extracellular space, and may thus be involved in regulating the quantal size [3–5].

It is now generally accepted that the presynaptic quantal size can change rapidly and very significantly as a result of stimulation or various pharmacological treatments [6–8]. Moreover the nature of secretory mechanism is such that the quantal size plasticity should generally be expected. First, the quantal size will change if the homotypic fusion changes [9]. Second, the quantal size should change because vesicles of different size are not equally efficient as barriers to diffusion of Ca^{2+} [10]. In all secretory systems, but especially in neuroendocrine cells with large vesicles and highly variable diameters, large vesicles will be released preferentially, but this is more pronounced when opening of Ca^{2+} channels becomes synchronous, as is the case during evoked release. Third, the fused vesicles may release only a fraction of their content ('kiss-and-run'; [11–13]. In such a case the quantal size should decrease at high release levels, due to incomplete re-filling of the vesicle. The importance of kiss-and-run mechanism however is presently hotly debated [14]. Finally, any

* Corresponding author. Tel.: +1 514 398 6002; fax: +1 514 398 7452.
E-mail address: mladen.glavinovic@mcgill.ca (M.I. Glavinović).

0005-2736/$ – see front matter © 2009 Elsevier B.V. All rights reserved.
doi:10.1016/j.bbamem.2009.01.018

change of the fusion pore dynamics may alter the postsynaptic quantal size irrespective of whether the release of the quantal content is complete or not [15].

Understanding mechanisms controlling the dynamics of exocytotic fusion pore dilatation and contraction is thus fundamental for understanding of quantal size plasticity. The cytoskeletal proteins may be considered as possible candidates controlling its dynamics [16]. They are known to play an important role in vesicular trafficking to the release sites. As a result of stimulation and calcium entry a depolymerization of the cortical actin network occurs facilitating exocytosis [17–19]. In this scenario the vesicular transport occurs by the action of molecular motors (such as myosin II) acting on F-actin trails. However, the molecular motors may also exert a tensional pressure on the F-actin network, which will alter the membrane tension, fusion pore expansion, and extrusion of vesicular contents [20]. Myosin II appears to act as a molecular motor on the fusion pore expansion by hindering its dilation when it lacks the phosphorylation sites, but the differences of the fusion pore dynamics and of the catecholamine release between control and transfected chromaffin cells with the unphosphorylatable form of myosin II are very limited [16]. Although their contribution may be greater in other secretory systems, it is necessary to consider the importance of other forces in regulating the dynamics of fusion pore dilatation.

In this study we focus our attention on the fluidic, electro-static and electro-kinetic forces acting on the fusion pore, and which are present simply because K^+ and glutamate$^-$ are extruded through the fusion pore. We simulate the fusion pore as a nano-sized cylinder with positively charged surface connected to two compartments equal in size using the computational methods of continuous nanofluidics [21–26]. The transmitter considered is glutamate, and it is negatively charged. K^+–glutamate$^-$ concentration in the vesicular compartment is either constant (stationary simulations) or changes in a step-like manner (time-dependent simulations). The extra-cellular compartment contains Na^+Cl^-, whose concentration does not vary during simulation. In most simulations the pressure and potential difference between two compartments are zero, whereas the surface charge density varies from one simulation to another over a wide range. Coupled system of Poisson–Nernst–Planck and Navier–Stokes equations is used to estimate the potential, electric field, pressure, fluid and ionic fluxes in the nanofluidic pore and to assess the forces acting on the fusion pore. Four forces are considered: a) inertial force, b) pressure, c) viscous force, and d) electrostatic force. The inertial and viscous forces are found to be very small, but the electrostatic force and force due to pressure may be significant. Counter-intuitively, the direction of both forces is often such to close the pore. The extrusion of the vesicular content thus by itself generates forces, which not only may affect the fusion pore dynamics, but more unexpectedly tend to close the pore. Moreover, the force generated by the extrusion of vesicular content can be sufficiently large to overcome forces caused by the tension difference between vesicular and plasma membrane.

2. Methods

2.1. Mathematical model

Poisson–Nernst–Planck (PNP) equations are used to calculate ionic current through a pore for all ionic species. PNP equations are composed of the Poisson (1) and Nernst–Planck (2) equations. The electrostatic potential (Φ) is calculated using Poisson equation:

$$-\nabla.\varepsilon_0\varepsilon_r\nabla\Phi = \rho_e \tag{1}$$

where ε_0 is the permittivity of vacuum, ε_r is the relative dielectric constant of solution. Note that the same equation applies to the membrane, but in the membrane the relative dielectric constant is ε_m, and the charge density ρ is zero. In solution the charge density ρ_e is given by:

$$\rho_e = F\sum z_a c_a \left(= e\sum z_a n_a\right) \tag{2}$$

where c_a is the molar concentration of ion a [mol/m^3], F is Faraday constant ($9.648*10^4$ C/mol), z_a is the valence of ion a, n_a is the number density of ion a. The following factors also influence the potential in the fusion pore: a) the fixed charges on the pore wall, b) the mobile charges inside the pore, and c) the charges in the solution and on control edges outside the pore.

The movement (by convection–diffusion–migration) of ionic species in the electrolytic fluid/solution is given by the Nernst–Planck equation:

$$\mathbf{J}_a = \mathbf{u}c_a - D_a\nabla c_a - m_a z_a F c_a \nabla\Phi \tag{3}$$

where $\mathbf{J}_a$ is molar flux [mol/m^2 s], D_a and m_a are diffusivity and mobility of ion a ($m_a = D_a/RT$), respectively; $\mathbf{u}$ is fluid velocity and F, R and T are Faraday constant, gas constant [8.315 Jl/(Kmol) and temperature (in Kelvin), respectively. Finally, the conservation of ionic mass of a dynamic problem is given by:

$$\frac{\partial c_a}{\partial t} + \nabla.\mathbf{J}_a = 0. \tag{4}$$

Note that the divergence operator is defined as:

$$\nabla.\mathbf{J} = \frac{1}{r}\frac{\partial}{\partial r}(rJ_r) + \frac{\partial J_z}{\partial z} \tag{5}$$

where J_r and J_z are the r- and z-components of vector $\mathbf{J}$.

The electrolytic fluid velocity $\mathbf{u}$ that is responsible for the convective transport of ions can be computed from the time dependent Navier–Stokes (NS) equations:

$$\rho\left(\frac{\partial\mathbf{u}}{\partial t} + \mathbf{u}.\nabla\mathbf{u}\right) = -\nabla p + \nabla.\left[\mu\left[\nabla\mathbf{u} + (\nabla\mathbf{u})^T\right]\right] + \mathbf{F}_e \tag{6}$$

$$\nabla.\mathbf{u} = 0. \tag{7}$$

Eq. (6) describes the conservation of momentum, while Eq. (7) accounts for the conservation of mass. In these equations ρ_f, μ, and p are respectively the density, viscosity and pressure of the fluid, while $\mathbf{F}_e$ is the electric force per unit volume ($\mathbf{F}_e = \rho_e\nabla\Phi$).

2.2. Geometry, parameters and boundary conditions

The nano-size fusion pore considered in this study has a cylindrical geometry. The computational domain describing this system consists of the fusion pore, a piece of the membrane wall as well as portions of the vesicular interior and extra-cellular spaces (Fig. 1A). The length of the pore L and of each of the compartments representing the vesicular and extra-cellular spaces was 10 nm resulting in total length of the computational domain of 30.0 nm. The fusion pore radius R ranged from 1.0 to 4.0 nm, whereas the radius W of the compartments representing the vesicular and extracellular spaces was 11 nm.

Axial symmetry condition has been applied on all variables along the axis of the fusion pore (boundary 4; Fig. 1B). The boundary conditions for the Nernst–Planck equation are concentrations of K^+–glutamate$^-$ and Na^+–Cl^- on two external controlling edges of the upper or vesicular compartment (boundaries 1) and lower or extra-cellular compartment (boundaries 2). On the edges of the upper compartment the concentrations of K^+–glutamate$^-$ ranged from 30 to 75 mM (mol/m^3), whilst the concentration of Na^+–Cl^- was 0 mM. On the edges of the lower compartment the concentration of K^+–glutamate$^-$ was 0 mM, while the concentration of Na^+–Cl^- was 150 mM. Note that we assume that: a) glutamate is negatively charged

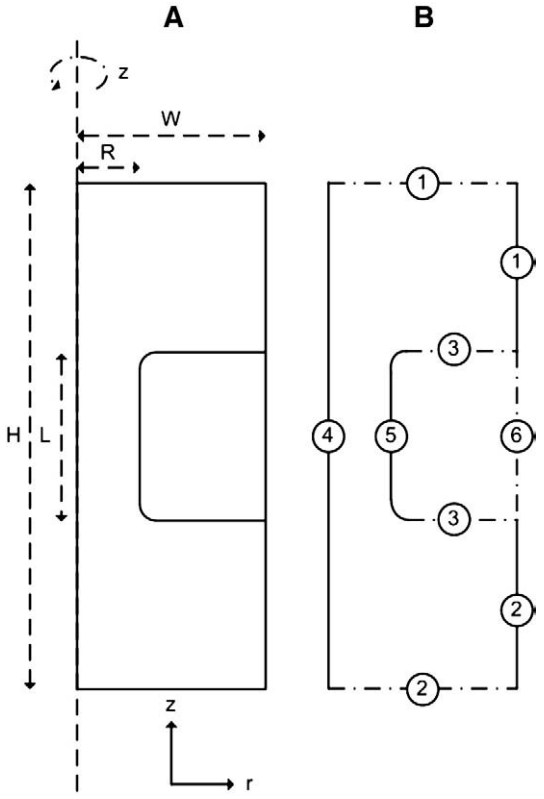

Fig. 1. (A) Semi-schematic of the hemi-section of the computational domain consisting of the cylindrical fusion pore and two compartments — an upper (vesicular) and a lower (extra-cellular) compartment. Three-dimensional model is generated by the rotation of the hemi-section about the central axis by 180°. Fusion pore radius R ranges from 1.0 to 4.0 nm (see Results), whilst the pore length L is 10 nm. The radius W of the compartments representing the vesicular and extracellular spaces is 11 nm. The total length of the computational domain including the fusion pore and two compartments is 30.0 nm. Finally the radii of curvature at the pore entrance and exit are set to 1.0 nm. (B) Axial symmetry condition was applied on all variables along the axis of the fusion pore (boundary 4). On two external controlling edges of the upper or vesicular compartment (boundaries 1) and lower or extra-cellular compartment (boundaries 2) the Nernst–Planck boundary conditions were concentrations of K^+–glutamate$^-$ and Na^+–Cl^-. K^+–glutamate$^-$ concentration ranged from 30 to 75 mM (mol/m^3), whilst Na^+–Cl^- was 0 mM ('upper' compartment). K^+–glutamate$^-$ was 0 mM, whilst Na^+–Cl^- was 150 mM/l ('lower' compartment). The Poisson boundary conditions were zero potential (both edges), or as otherwise stated, whereas the pressure (Navier–Stokes boundary condition) was 10–1000 kPa ('upper' compartment) and 0 Pa ('lower' compartment). At the solution–membrane interface (boundaries 3 and 5) the Nernst–Planck boundary condition was insulation/symmetry whereas the Navier–Stokes boundary condition was no-slip. The Poisson boundary condition was surface charge, which was either 0 (boundary 3) and $4*10^{-3}$ C/m^2 to $64*10^{-3}$ C/m^2 (internal wall of the fusion pore including the curved parts on both ends; boundary 5).

(see below), with a single negative charge, which remains constant throughout simulations, b) glutamate is simply considered as an ion (anion; i.e. the complexities of its shape are ignored), and c) the positive ion in the vesicle is potassium [26].

At the solution–membrane interface (boundaries 3 and 5) an insulation/symmetry or zero current condition was imposed. The boundary conditions (boundaries 1, and 2) for the Poisson equation were zero potential on both upper and lower controlling edges, or as otherwise stated. On the internal wall of the fusion pore (including the curved parts on both ends; boundary 5) the surface charge densities (σ) ranged from $8*10^{-3}$ to $64*10^{-3}$ C/m^2, which amounts to 3.9 and 30.8 unitary charges respectively for a 1 nm radius nanopore (or 14.3 and 114.6 unitary charges for a 4 nm nanopore). These values are comparable to those estimated for the cell membrane (one elementary negative fixed charge per 1–4 nm^2, which is equivalent to a charge density of 0.04–0.16 C/m^2; [27,28]). Note however that in this study the pore wall is considered to be positively charged. The surface charge density was 0 C/m^2 on the membrane exterior walls (boundary 3). Finally, a no-penetration and no-slip condition was imposed on the solution–membrane interface (boundaries 3 and 5), or as otherwise specified. The pressure difference between the controlling edges of the upper (boundaries 1) and lower (boundaries 2) compartments varied from 10^4 Pa to 10^6 Pa (Navier–Stokes boundary conditions; see Results). Since the pressure at the controlling edges of the lower compartment is assumed to be zero all values are relative to it. The 'absolute' pressure can be estimated from molecular dynamics simulations. Both the thermal motion and pairwise atomic interactions contribute to it.

The system of coupled equations given by the PNP and NS equations was solved by finite element method with adaptive mesh refinement, and using a commercial software package program Comsol 3.4 (Comsol, Burlington, MA, USA), whereas the post-processing was performed using a software package for scientific and engineering computing Matlab (MathWorks, Natick, MA, USA). The mesh independence of the solutions was verified using standard procedures. The diffusion coefficients for ions diffusing freely in bulk aqueous solution are well known [29,30], but it is less clear what they may be in the confined space of the fusion pore, where the electrostatic and non-electrostatic interactions with the walls of the fusion pore [24,31] will restrict ion motion and reduce the diffusion coefficients. We make a simplifying assumption that all diffusion coefficients are isotropic, spatially uniform and the same as in the aqueous solution. Similar assumption is made about the dielectric constant and viscosity. The relative dielectric constants of the membrane (ε_m) and solution (ε_s) were 2 and 80 respectively. The diffusion constants of Na^+, Cl^-, K^+ and glutamate$^-$ were $1.33*10^{-9}$, $2.03*10^{-9}$, $1.96*10^{-9}$, and $0.76*10^{-9}$ m^2/s, respectively (or were reduced by 90% but only in the nanopore), the viscosity of the fluid was typically 1 mPas, but in some simulations it ranged from 0.5 mPas to 4 mPas, whereas the temperature was always 300K (see Results).

The electrical recordings of the fusion pores and ion channels are similar [1]. The ion channels are formed of well-characterized proteins, but it is less well known what the structural components of the fusion pore are. Recent studies suggest that the fusion pore incorporates soluble *N*-ethylmaleimide-sensitive factor attachment protein receptors (SNAREs) [32,33], and is thus envisioned as a lipoprotein. The protein part consists of a chain of amino acids folded to form a water-filled nanopore controlling the transport of transmitter. The charge on proteins arises from some of the amino acid side chains, the amino and carboxy-termini, and bound ions. The charge on amino acid side chains depends on the pK_A of the side chains but also on the pH of the solution. When the pH is greater than the pK_A of a group, the deprotonated form predominates, giving acidic side chains a charge approaching −1 and basic side chains a charge approaching 0. However, when the pH is less than the pK_A of a group, the protonated form of the group predominates leaving the acidic side chains with a charge close to 0 and the basic side chains with a charge near +1. The charge density on the wall of the fusion pore will thus be at least partly determined by the pH of the solution in the pore, and should change depending on the vesicular, or extracellular pH. Vesicular interior is acidified prior to release [34], and the fusion pore will be positively charged, although the charge density will vary as pH changes during release as vesicular and extra-cellular solutions come into contact. Similar reasoning applies to glutamic acid. The intra-vesicular pH in chromaffin cells has been reported to be ~5.6 [35–38], whereas at hippocampal nerve terminals it is ~5.5 [39]. Given that pK_A of the α-COOH of the glutamic acid is 2.19, and of its R-group it is 4.25 [40] glutamic acid will be negatively charged. The lipid content of the pore will rise with pore dilatation, possibly becoming a prevailing component of the pore wall, and the negative charge on the phosphatidylserine will modify the charge density on the pore wall previously determined by the protein charges.

2.3. Assumptions of continuum modeling of glutamate$^-$ and ion transport in charged nanopores

The classical Poisson–Nernst–Planck equation we use is derived assuming that the ions are infinitesimal. Moreover, the ion–ion, ion–water and ion–wall interactions are all considered in a mean-field fashion, and the molecular aspects of these interactions are ignored. Navier–Stokes equations assume that the fluid density does not vary significantly over intermolecular distances. However, recent molecular dynamics simulations suggest that the ion and molecular (water and glutamate) distributions near the pore wall are influenced by their discreteness and finite size, ion–wall and ion–molecule interactions [41–43]. Such contributions may be important for very narrow pores but they are beyond the scope of this study. Additional limitations of PNP theory may arise if the pore is very narrow, when its radius is smaller than the Debye length [44], because the dielectric self-energy contribution to the ion's potential energy is not taken into account. The inclusion of an explicit self-energy term in the formalism remedies this problem, but in the present study the radius of the fusion pore is typically significantly greater than the Debye length and the contribution of the dielectric self-energy was ignored.

3. Results

3.1. Effect of vesicular K^+ and glutamate$^-$ concentrations, pressure and potential on steady-state force acting on pore wall

Fig. 2C–F depicts how the steady-state forces (inertial, viscotic, pressure, electrostatic as well as total) acting on the pore wall in the radial direction depend on the vesicular K^+ and glutamate$^-$ concentration (or more precisely on the concentration at the controlling edges of the upper compartment; see Fig. 1). Irrespective

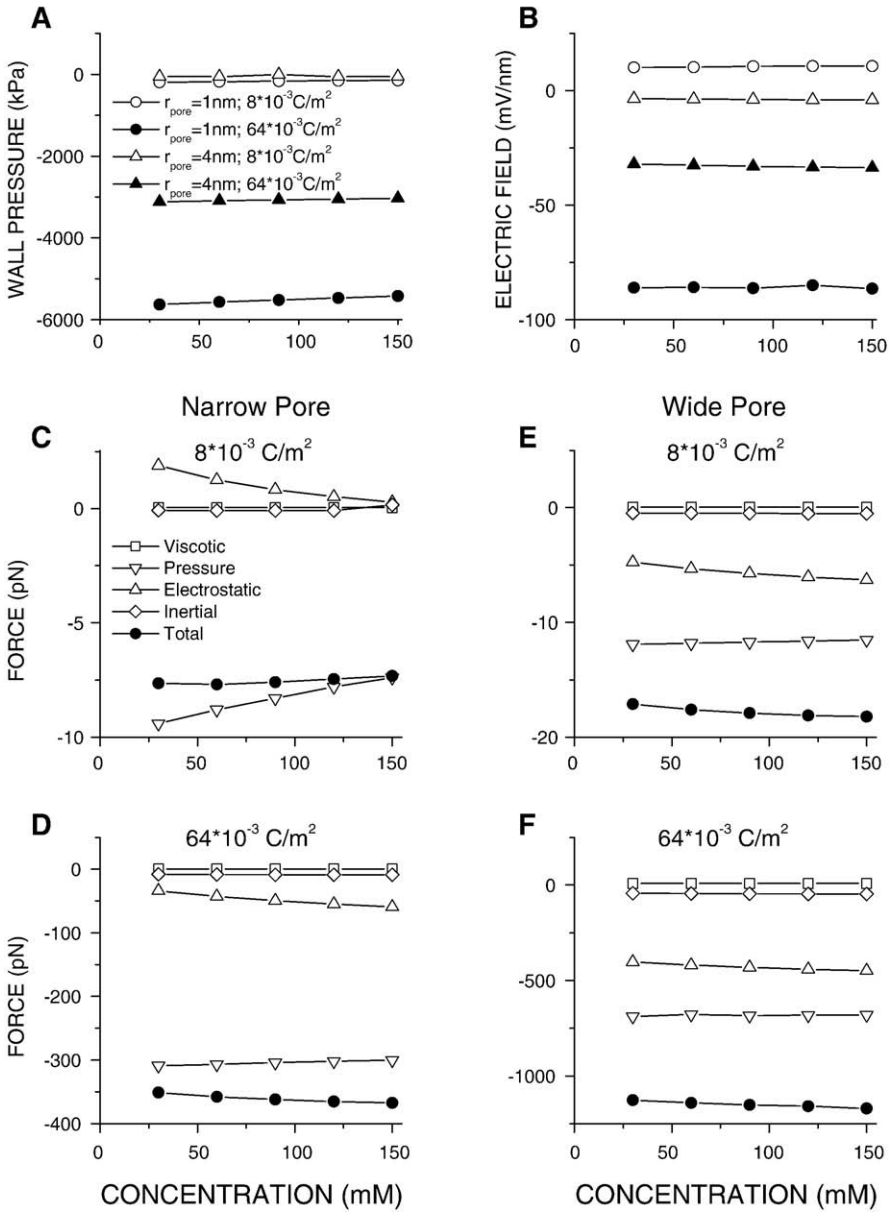

Fig. 2. (C–F) Steady-state pore wall total radial force is largely independent of the vesicular K^+–glutamate$^-$ concentration irrespective of the pore radius or pore wall charge density and tends to close the pore. The electrostatic force tends to open the pore when the pore is narrow and pore wall charge density low, and to close it when the pore widens or pore wall charge density increases. Both the electrostatic force and pressure force increase greatly as pore wall charge density rises, and increase but moderately when the pore dilates. (A–B) Wall pressure rises moderately, whereas the radial electric field at the pore wall center (i.e. mid-way between the upper and lower compartment) is insensitive to the rise of the vesicular K^+–glutamate$^-$ concentration. The vesicular pressure was 0 Pa, whereas the potential was 0 mV.

of whether the charge density on the pore wall is low ($8*10^{-3}$ C/m^2) or high ($64*10^{-3}$ C/m^2), or whether the pore is narrow (1.0 nm radius) or wide (4.0 nm radius) the forces are largely independent of the K^+–glutamate$^-$ concentration. More importantly the direction of the total force is in all cases toward the pore center (i.e. to close the pore). Note also that the inertial force and the force due to the viscotic interaction of water and pore wall are both very small. The electrostatic force is positive (i.e. it tends to open the pore) but very small, only when the pore is narrow and the pore wall charge density low. The force is positive owing to the fact that the charges on the pore wall, which are radially on the opposite side, are close to each other. This repulsive force prevails, though only marginally, over the attractive force between the pore wall charges and the ions in the pore (which are overwhelmingly counter-ions). Otherwise it is negative and thus acts to close the pore. In this simulation the force due to the pressure is entirely electro-kinetically driven (the intra-vesicular pressure is zero). Nevertheless, the pressure makes the greatest contribution to the total force on the pore wall. It is also always negative and always acts to close the pore. Most importantly the electrostatic force and pressure force both increase greatly when the charge density on the pore wall rises, and to a lesser extent when the pore dilates.

The pressure–force at the pore wall is an integral of pressure contributions from all points at the pore wall (see Appendix). If the pore radius changes the pressure force will change because of change of geometry (change of the surface area of the pore wall). However, the pressure force may also change because the pressure at the wall changes (i.e. because of change of physics). To assess such contributions to the pressure-force we also estimated the pressure at the wall at a single point in the pore center. This is a simple test, but provides a quick insight into the nature of the changes. It is clear that the pore wall pressure strongly depends on the pore radius and wall charge density, but does not depend on K^+–glutamate$^-$ concentration (Fig. 2A). Similar dependence is observed when the relationship between the electrical field and K^+–glutamate$^-$ concentration, or pore radius and charge density are examined (Fig. 2B).

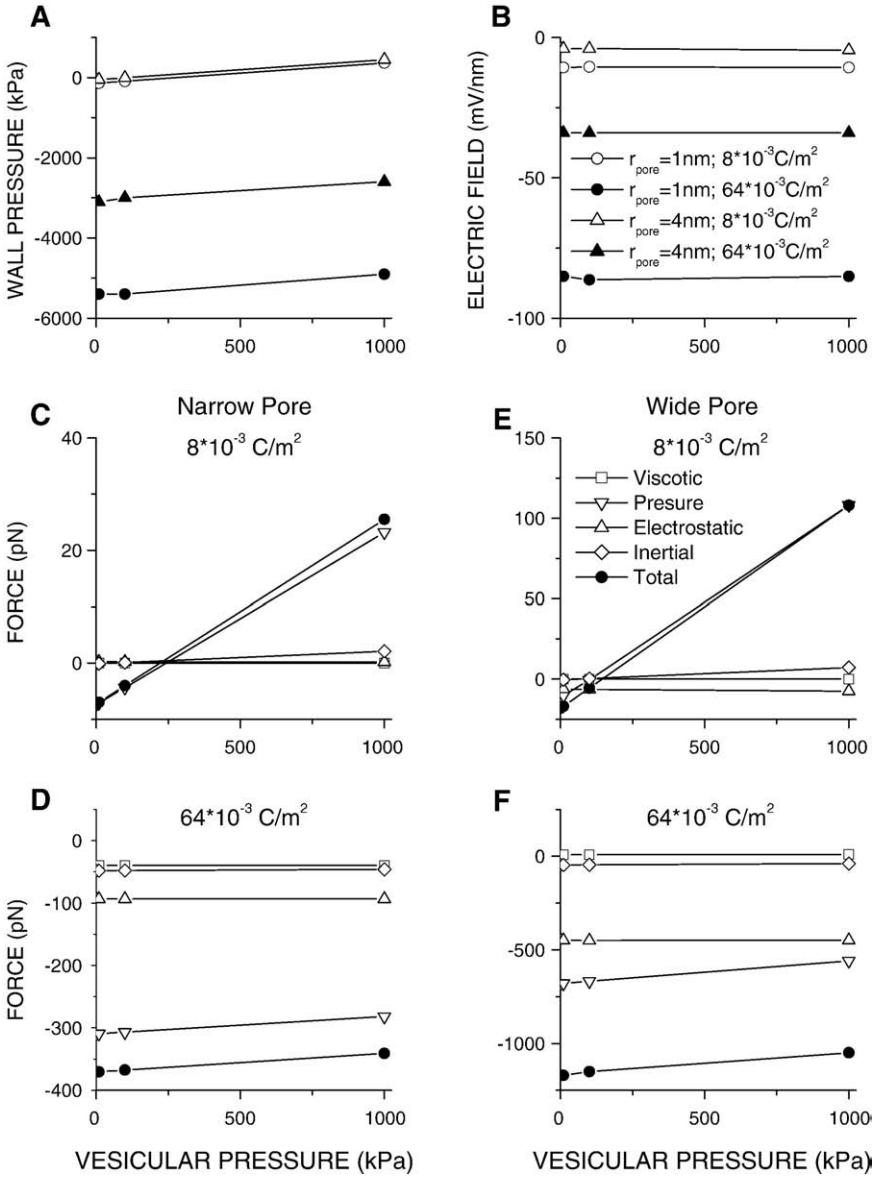

Fig. 3. (C and E) Vesicular pressure largely determines the steady-state total wall radial force if the pore wall charge density is low and vesicular pressure high, and tends to open the fusion pore. (D and F) Its contribution can predominate if the pore is wide and its wall charge density low, but if the charge density is high the induced pressure becomes much greater, the force on the pore wall becomes large and negative and together with large and negative electrostatic force acts powerfully to close the pore. (A–B) As the vesicular pressure rises the pore wall pressure at the center rises marginally, but the radial electric field does not. The K^+–glutamate$^-$ on the controlling edges of the upper compartment was 150 mmol/l, and the potential was 0 mV.

Both the vesicular pressure and electro-kinetically induced pressure influence the pressure and pressure force on the pore wall, but their contributions change depending on the geometry and physics of the situation. Fig. 3C–F shows how the radial steady-state forces (total force, pressure but also inertial, viscotic and electrostatic forces) acting on the wall of the fusion pore depend on the intra-vesicular pressure for a narrow and wide pore, and with charge density low or high. If the intra-vesicular pressure is moderate to high (200–1000 kPa), and the charge density on the pore wall is low, and irrespective of the pore radius the total radial force acting on the pore wall is positive and tends to open the fusion pore (Fig. 3C–E). The radial force due to the pressure clearly predominates, whereas the contributions due to the radial inertial, viscous but also the electrostatic force are very small. When the charge density on the pore wall rises, the contribution of various radial forces acting on the pore wall changes significantly (Fig. 3D and F). Note that when the charge density is high, the pressure-force becomes large and negative and essentially independent of the vesicular pressure. It is thus not the vesicular, but electro-kinetically driven pressure that determines the pressure-force. The radial force due to the electrostatic interactions ('electrostatic force') also becomes large and negative, and both forces (electrostatic force and pressure-force) thus act powerfully to close the pore. Note however, that the wall pressure and electric field are largely independent of vesicular pressure irrespective of the pore radius and charge density on the pore wall (Fig. 3A–B). The insensitivity of the wall pressure on vesicular pressure in a narrow pore with low charge density contrasts with strong dependence of the pressure force on vesicular pressure, and suggests that the axial pressure gradient is steep.

It may be argued (see Discussion) that the radial forces acting on the pore wall could depend on the potential difference between the upper ('vesicular') and lower ('extra-cellular') compartments, which may arguably affect the flux and spatial distribution of charged particles and thus water velocity and pressure. However, the effect is clearly very limited for the range of potential differences likely to be encountered physiologically (Fig. 4C–F), although a very modest dependence is visible, but only when the pore is narrow and charge

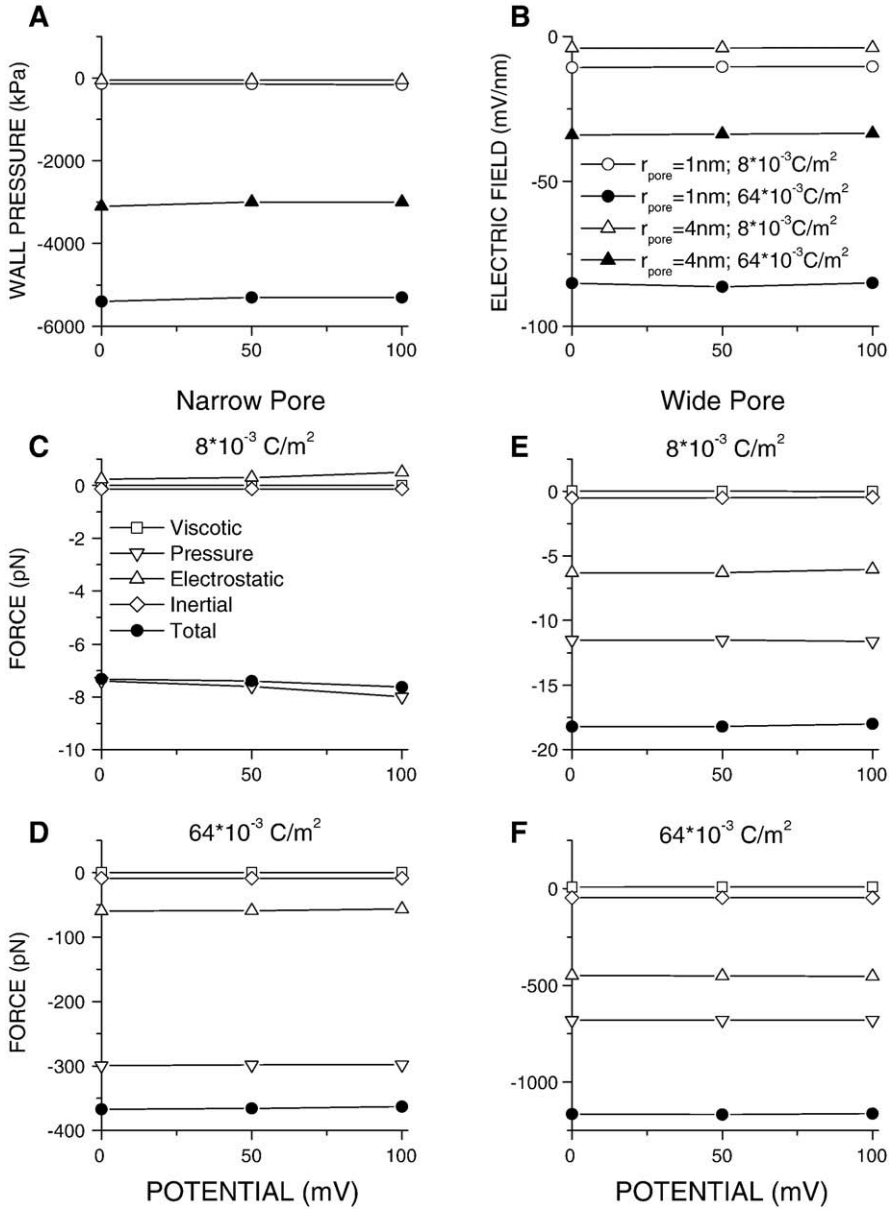

Fig. 4. (C–F) Potential difference between 'vesicular' and 'extracellular' compartments has very little influence on the force acting to open or close the pore, irrespective of the pore radius or pore wall charge density. (A–B) Both the pressure and the radial electric field at the pore wall in its center are insensitive to this potential difference. The K^+–glutamate$^-$ on the controlling edges of the upper compartment ('vesicular concentration) was 150 mmol/l, whereas the pressure was 0 Pa.

density on the pore wall low (Fig. 4C). Finally, neither the wall pressure, nor the wall electric field at a single point in the pore center clearly, depend on the vesicular pressure irrespective of the pore radius or charge density on the wall (Fig. 4A–B).

3.2. Pore wall charge density critically influences force acting on pore wall whereas diffusion constant of ions and glutamate$^-$ and water viscosity have only marginal effect

Figs. 5 and 6 depict how various factors in the pore (rather than those originating from the vesicle) influence the radial force acting on the pore wall. The results already shown demonstrate that the charge density on the pore wall is important, but a direct evaluation of how the radial force depends on the charge density shows that it is, and by far, the most important 'physical' factor, irrespective of whether the pore is narrow or wide (Fig. 5C–D). It strongly influences the electro-kinetically induced pressure, which is always negative. As expected it also determines the electrostatic force in the radial direction, which though smaller than pressure-force, is also important. The sign of the electrostatic force depends on the pore radius. If the pore is narrow and the charge density is low the electrostatic force is marginally positive. Being smaller than the radial pressure-force, it reduces the total force. If the charge density is moderate or high the electrostatic force becomes negative and reinforces the negative pressure force. When the pore is wide both the electrostatic force and pressure-force are negative irrespective of the charge density on the pore wall, reinforce each other and provide a powerful force to close the pore. It is known that Ca^{2+} stores build-up in synaptic and dense core vesicles, that vesicular Ca^{2+} is extruded through the fusion pore and that it may trigger

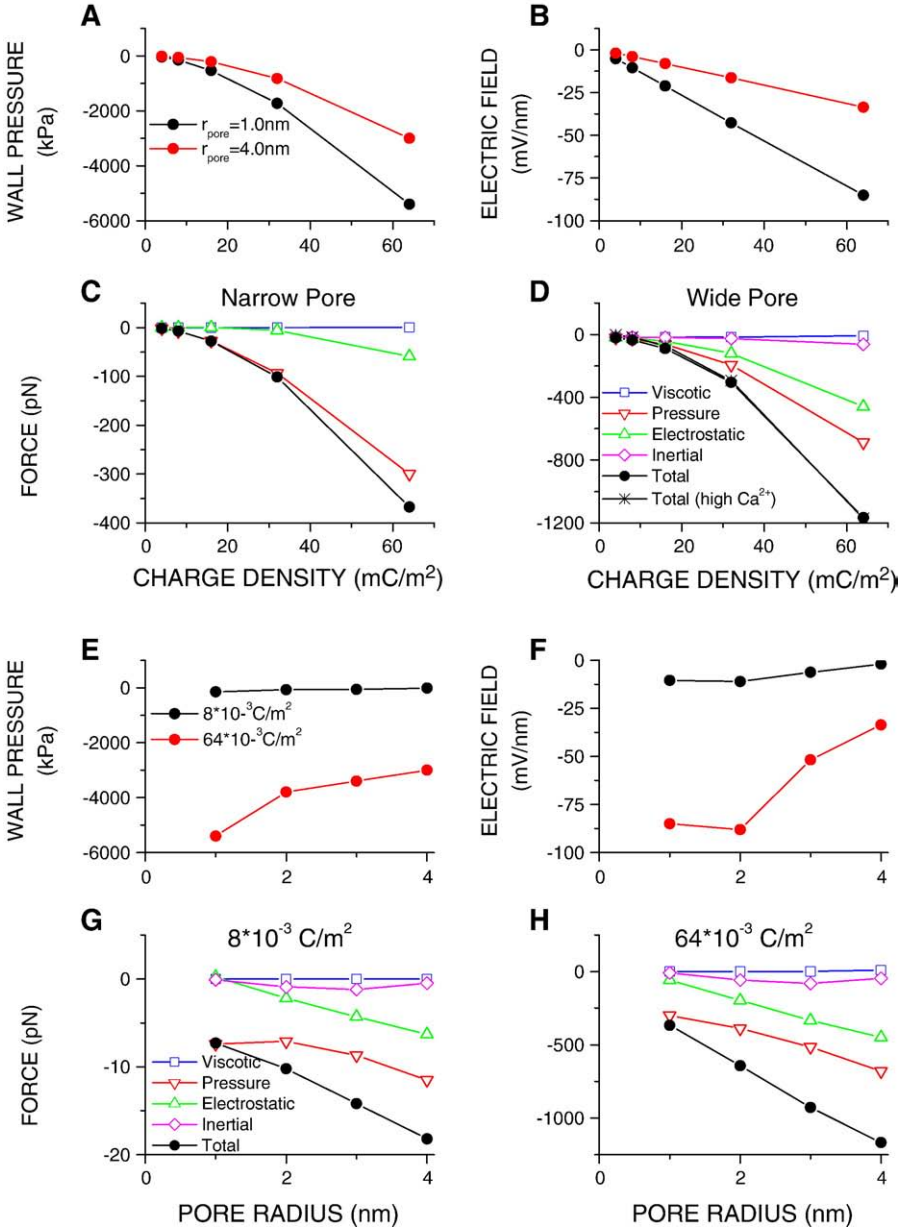

Fig. 5. (C–D) Pore wall charge density influences greatly the pore wall radial force by determining the electrostatic force and pressure force. As charge density rises the electrostatic force rises and its direction is outward (positive) if the pore is narrow, but in the wide pore it is much higher and inward (negative). Moreover, the pressure force in both cases becomes markedly more negative. Note that the total force (wide pore) does not change if in addition to K^+–glutamate$^-$ (150 mM) $CaCl_2$ (32 mM) is also present on the controlling edges of the vesicular compartment. (A–B) In addition, both the wall pressure and the radial electric field in its center become more negative. Both are also much smaller for a wide pore. (G–H) All pore wall forces (the total force and its two dominant components — electrostatic and pressure force) become more negative as the pore dilates, irrespective of the wall charges. (E–F) Both wall pressure and radial electric field in its center become less negative with pore dilatation, especially if the pore wall charge density is high.

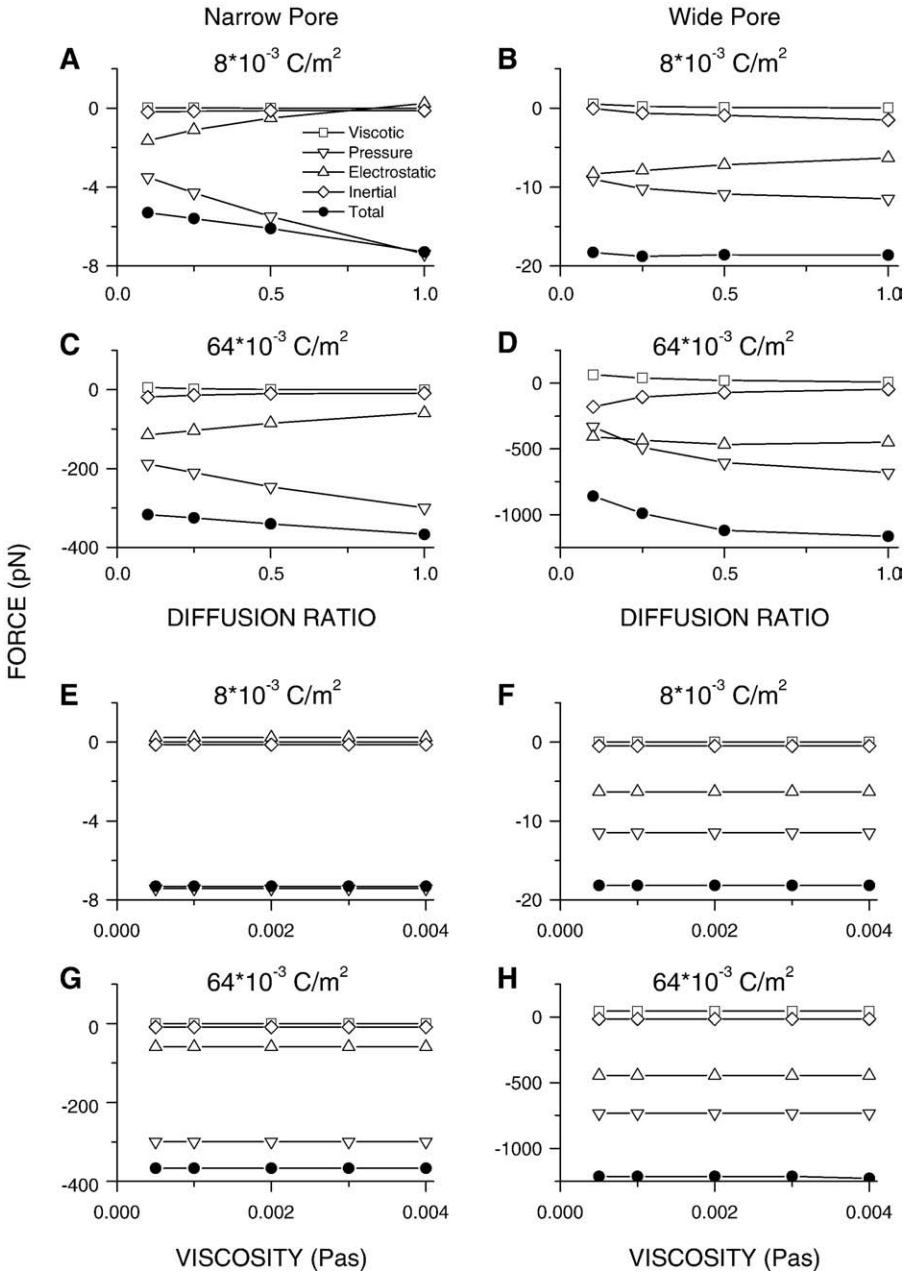

Fig. 6. Pore wall force does not depend greatly on the diffusion constants of charged particles or water viscosity. (A–D) Lowering the diffusion constants of K^+, glutamate$^-$, Na^+ and Cl^- by 90% renders the wall force modestly less negative, and the less negative pressure force is partially counter-balanced by the more negative electrostatic force. Diffusion ratio of one indicates the diffusion constants as in the bulk solution. (E–H) The total wall force and all of its components (viscotic force, electrostatic force and pressure force) also do not change if the water viscosity is reduced by up to 87.5%. K^+–glutamate$^-$ vesicular concentration was 150 mmol/l, the pressure was 0 Pa and the potential was 0 mV.

exocytosis of additional vesicles [45]. As our simulations show the Ca^{2+} presence on the controlling edges of the vesicular compartment, (even at high concentration; 32 mM) in addition to 150 mM of K^+–glutamate$^-$, will not affect the total force acting on the pore walls (Fig. 5D).

As already stated the charge density on the pore wall or pore radius have a 'direct' effect on the force on the pore wall, since they determine the amount of charge on the wall and its surface area, but the 'indirect' effects due to change of 'physics' of the situation are also important. The wall pressure in the pore center becomes more negative (and supra-linearly) as the pore wall charge density rises, and the effect is more pronounced when pore is narrow (Fig. 5A). The radial component of the wall electric field also becomes more negative as the charge density rises, but linearly, and the slope is greater for a narrow pore (Fig. 5B). Note however, that the wall pressure and radial electric field do not depend on pore radius if charge density is low, but both become less negative if charge density is high (Fig. 5E–F). Finally, the radial force on the pore wall vs. pore radius relationship for two different charge densities at the pore wall is shown in Fig. 5G–H. As expected the inertial and viscotic forces are always quite small. The pressure-force is always negative and strongly (supra-linearly) depends on the pore radius. The electro-static force is marginally positive when the charge density on the pore wall is low and pore is narrow, but otherwise it is negative, and its value increases linearly with pore radius.

Given that the diffusion constants of ions and molecules, and water viscosity may be very different in the confined space than in the bulk solution [43,44,46] we evaluated whether their changes would significantly affect the force on the pore wall, but this was not the case. Reducing the diffusion constant of ions (Na^+, K^+ and Cl^-) and

glutamate$^-$ in the pore by 90% (in each case all diffusion constants were reduced to the same extent) had a limited effect (Fig. 6A–D). Changing the water viscosity in the fusion pore from 0.5 mPas to 4 mPas had essentially no effect on the radial total force, or on any of the forces contributing to it (Fig. 6E–H). Note that outside of the fusion pore the diffusion constants of ions and glutamate$^-$ and water viscosity remained as in the bulk solution.

3.3. Spatial distributions of K^+ and glutamate$^-$, but also of Na^+ and Cl^- within the pore change as vesicular K^+–glutamate$^-$ concentration rises

K^+ and glutamate$^-$ concentration in the upper compartment influences their concentration in the fusion pore. Whereas their concentration levels can be estimated using stationary simulations, time-dependent simulations are needed to estimate the time needed to reach new levels following a change in the concentration. Fig. 7A–D depicts how the radial and axial profiles of both K^+ and glutamate$^-$ concentration change in the vesicular compartment and within the 'narrow' pore ($r_{pore} = 1.0$ nm), when their concentrations at the controlling edges rise from 30 to 75 mmol/l. In the vesicular compartment K^+ concentration rises rapidly to the values at the controlling edges. The change extends into the pore though only to a limited extent, being more pronounced in the center (K^+ is a co-ion; Fig. 7A–B). Glutamate$^-$ concentration in the vesicular compartment also rises rapidly. Prior to the vesicular concentration change the glutamate$^-$ concentration in the pore is much above the vesicular concentration owing to the electrostatic interactions and the fixed charges at the pore wall (glutamate$^-$ is considered as a counter-ion). Following the step-like rise of vesicular K^+ and glutamate$^-$ concentrations, the glutamate$^-$ concentration within the pore rises to even higher levels especially close to the pore wall. Interestingly the change of the vesicular K^+–glutamate$^-$ concentration also results in the concentration change of Na^+ and Cl^- within the pore, although their extra-cellular concentration is kept constant, but the change is modest. Whereas Na^+ concentration rises Cl^- concentration diminishes (Fig. 7E–H). If the pore is wide the changes of the spatial

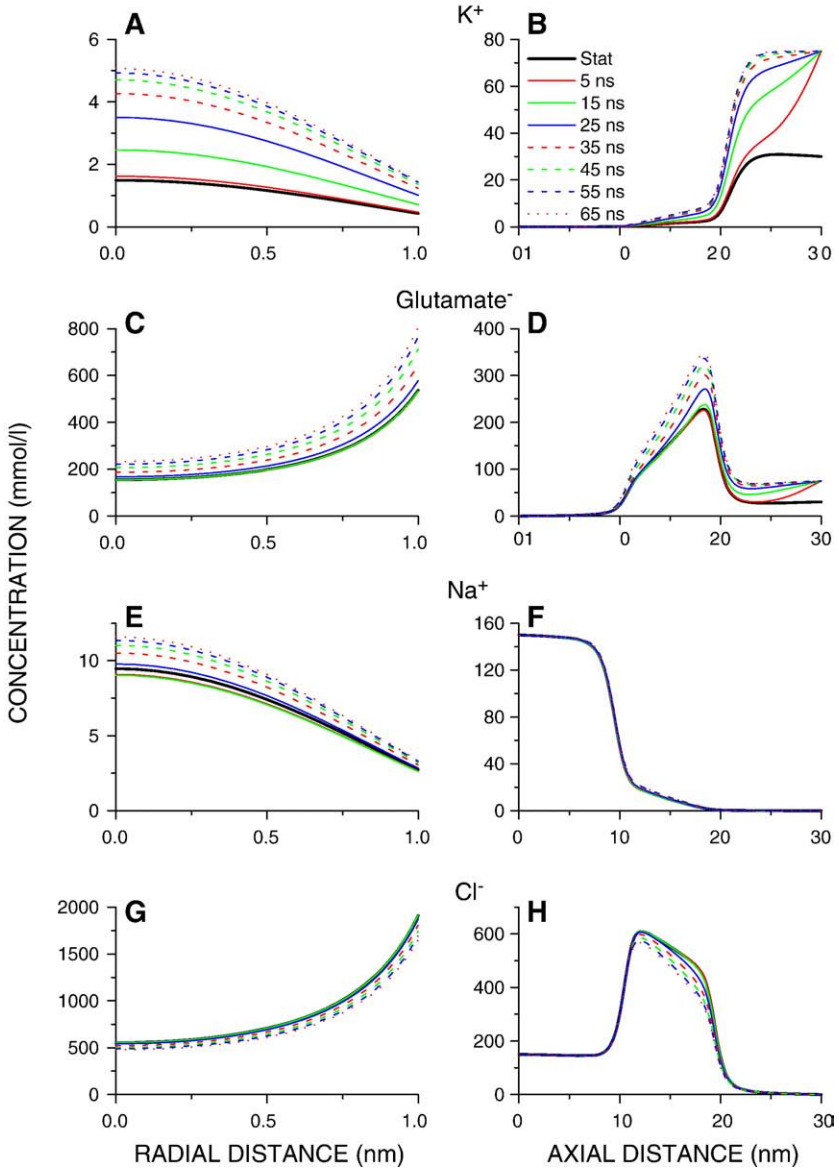

Fig. 7. (A–D) Spatial profiles (radial and axial) of both K^+ and glutamate$^-$ concentration change, when their vesicular concentration rises (from 30 to 75 mmol/l). Within the pore K^+ concentration (which is very low; K^+ is a co-ion), and glutamate$^-$ concentration (which is very high; glutamate$^-$ is considered as a counter-ion) both rise. E–H) Interestingly Na^+ and Cl^- concentrations change too though modestly, although their extra-cellular concentration is constant (at the controlling edges). Na^+ concentration rises whereas Cl^- concentration diminishes. Vesicular pressure was 0 Pa and the potential was 0 mV.

distributions of K^+, Na^+, Cl^- and glutamate$^-$ concentrations are qualitatively the same as those for the narrow pore but are less pronounced (not shown).

3.4. Spatial distributions of water velocity and potential change whereas charge density and pressure remain constant following rise of vesicular K^+–glutamate$^-$ concentration

Vesicular K^+–glutamate$^-$ changes induce also a chain of events to alter other variables — fluidic, electro-kinetic and electro-static. Water velocity changes quite significantly (Fig. 8A–B). The shape of velocity distributions remains largely the same but the values are altered. Water velocity rises initially, before diminishing to a new lower steady-state level (positive velocity indicates the efflux or outward movement of water). In contrast the pressure, which is entirely electro-kinetically driven (vesicle to extra-cellular pressure difference is zero), is altered only marginally. It is very negative near the pore wall owing to the relatively high charge density on the pore wall ($64*10^{-3}$ C/m^2; Fig. 8C–D). The most important finding is that the spatial profiles of the charge density in the pore remain essentially un-altered following the step-like rise of vesicular K^+–glutamate$^-$ concentration, although the K^+, Na^+ and Cl^- and glutamate$^-$ concentrations in the pore change quite significantly (Fig. 8E–F).

Note that in the pore the potential is quite high although the vesicle to extra-cellular potential difference is zero. Along the central axis of the pore the potential reaches ~+60 mV, and near the wall it rises to more than 80 mV. The potential results from the presence of the fixed charges on the pore wall, which are only partially counter-balanced by the presence of ions and glutamate$^-$ in the pore. Finally, although the charge density in the pore changes only marginally following a step-like vesicular K^+–glutamate$^-$ concentration change the potential in the pore changes albeit modestly (by ~10 mV), becoming more depolarized before settling to a new lower level (Fig. 8G–H). Even marginal changes of the pore charge density thus affect the potential in the pore. Finally, if the pore is wide the velocity, pressure, charge density and potential profiles will change in a qualitatively similar manner (not shown).

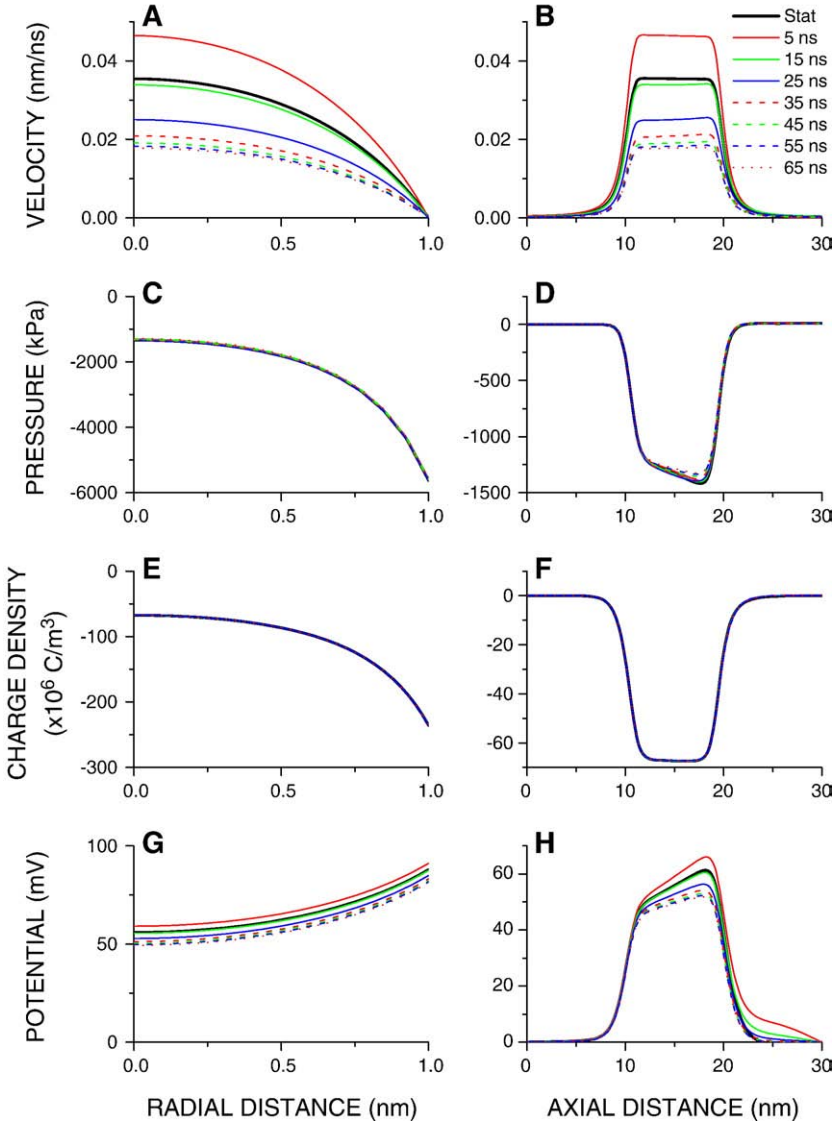

Fig. 8. Change of the radial and axial profiles of the water velocity, pressure, pore charge density and potential in a narrow pore induced by the step-like rise of the vesicular K^+–glutamate$^-$ concentration (from 30 to 75 mmol/l). (A–B) Water velocity first rises, before diminishing to a new lower steady-state level. Negative velocity indicates the outward movement of water. (C–D) The pressure, which is entirely electro-kinetically driven (vesicular pressure is zero), is very negative near the pore wall, and changes only marginally, if the vesicular concentration rises. (E–F) Radial and axial profiles of the pore charge density do not change. (G–H) Potential profiles (radial and axial) become more depolarized, before settling to levels below original levels (i.e. to more hyper-polarized levels), but the change is small. Vesicular pressure was 0 Pa and the potential was 0 mV.

3.5. Change of pore mean concentration of K^+, glutamate$^-$, Na^+ and Cl^- and of water velocity following a step-like rise of vesicular K^+–glutamate$^-$ concentration

For a quick comparison of the ion concentrations, water velocity, potentials and charge density over different geometries or under different conditions it is desirable to evaluate their mean values. Fig. 9A–B depicts the change of the mean K^+ concentration in the pore following a step-like rise of the K^+–glutamate$^-$ concentration on the upper controlling edges from 30 to 75 mmol/l. The mean K^+ concentration rises rapidly from a low to a higher level (K^+ is a co-ion). The half-time is 25 ns ('narrow pore'; Fig. 9A), and 26 ns ('wide pore'; Fig. 9B). The rise of the mean glutamate$^-$ concentration in the pore is similarly rapid, but occurs from a higher level (glutamate$^-$ is simulated as a counter-ion). Its rise half-time is 36 ns ('narrow pore') and 37 ns ('wide pore'). Interestingly, both Na^+ and Cl^- concentrations also change, although their concentration on the controlling edges of the lower compartment ('extra-cellular concentration') does not change, and the change is relatively greater when the pore is narrow. Na^+ concentration decreases before rising to a new steady-state level irrespective of the pore width, whereas Cl^- concentration decreases. The half-time is 37 ns (Na^+; 'narrow pore'), 45 ns (Na^+; 'wide pore'), 45 ns (Cl^-; 'narrow pore'), 45 ns (Cl^-; 'wide pore'). In contrast the charge density and number of charges within the narrow (Fig. 9C–D) or wide pore (Fig. 9E–F) are completely unaffected by the changes of K^+–glutamate$^-$ concentration on the edges of the upper compartment, although such a change alters significantly the concentration of all charged particles (K^+, Na^+ and Cl^- ions and glutamate$^-$).

Given a concentration gradient of ions and glutamate$^-$ between the vesicular and extra-cellular compartments, which results in their flux,

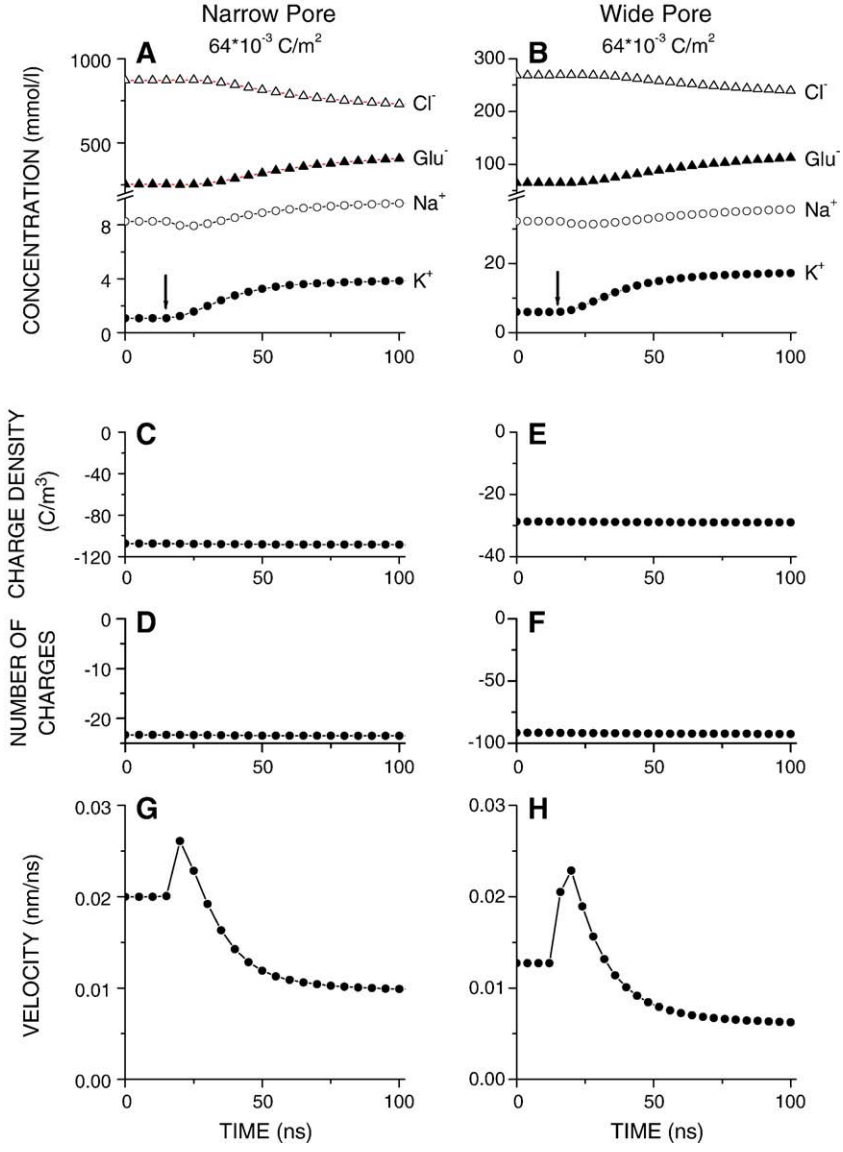

Fig. 9. (A–B) Mean pore K^+ concentration rises rapidly from a low level (K^+ is a co-ion), when the vesicular K^+–glutamate$^-$ concentration rises from 30 to 75 mmol/l. The half-time is 25 ns ('narrow pore'), and 26 ns ('wide pore'). Mean pore glutamate$^-$ concentration also rises, but more slowly and from a higher level. The corresponding half-times are 36 ns ('narrow pore') and 37 ns ('wide pore'). Na^+ and Cl^- also change especially if the pore is narrow, although their extracellular concentration did not change. The half-times for Na^+ are 37 ns ('narrow pore') and 45 ns ('wide pore'), whereas for Cl^- they are 45 ns for both the narrow and wide pore. Na^+ concentration decreases before rising to a new steady-state level in the narrow and wide pore. In contrast the charge density and the number of charges within the narrow (C–D) or wide pore (E–F) do not depend on the changes of the vesicular K^+–glutamate$^-$ concentration, although such a change alters significantly the concentration of K^+, glutamate$^-$, Na^+ and Cl^-. (G–H) Water velocity however, changes significantly and biphasically from a non-zero stationary level. The half-times for water velocity changes are 21 ns ('narrow pore') and 26 ns ('wide pore'). Positive water velocity indicates its efflux from the upper (vesicular) compartment. First arrow indicates the onset of the step-like change of the vesicular concentration. Vesicular pressure was 0 Pa and the potential was 0 mV.

the net flux of water under stationary conditions is not surprising (Fig. 9G–H). Any change of the vesicular K^+ and glutamate$^-$ concentration should thus be associated with a change of the velocity of water, and that was the case too. Irrespective of whether the vesicular K^+–glutamate$^-$ concentration was 30 or 75 mmol/l, the water flow was out of the vesicle. As a result of the vesicular K^+–glutamate$^-$ concentration change the water velocity initially rose from its steady-state value before diminishing to a new but lower level. It is interesting to note that whereas the steady-state mean velocity of water is greater for a narrow pore, its transient change is more pronounced for a wide pore. The half-time is 21 ns ('narrow pore') and 26 ns ('wide pore').

3.6. Efflux of K^+ and glutamate$^-$ and influx of Na^+ increases whereas influx of Cl^- decreases as vesicular concentration of K^+–glutamate$^-$ rises

Even when the vesicular pressure is zero and in the absence of any potential difference between the controlling edges of the vesicular and extra-cellular compartments the flux of charged particles (K^+, Na^+, Cl^- and glutamate$^-$) should not be entirely diffusive. The electrical field caused by the presence of fixed charges on the pore wall and the presence of charged particles (Na^+, K^+ and Cl^- and glutamate$^-$) within the pore will generate the migratory flux of these ions and glutamate$^-$. The flux of charged particles will produce water movement, and thus a convective flux of ions and glutamate$^-$. Fig. 10 depicts the diffusive, migratory, convective fluxes and the total fluxes of K^+, glutamate$^-$, Na^+ and Cl^- for a narrow ($r_{pore} = 1.0$ nm) and wide ($r_{pore} = 4.0$ nm) pore. In each case the fluxes (number/μs) are shown on the right ordinate, whereas the corresponding unitary fluxes (number/nm^2 μs) are shown on the left ordinate. Irrespective of whether the pore is narrow or wide the convective fluxes of ions and glutamate$^-$ are very small. Given that the vesicular pressure was zero this is not surprising. Diffusive flux is typically the most important, but the migratory flux of Cl^- becomes comparable to its diffusive flux. Finally, note that all fluxes of the co-ions (K^+ and Na^+) are smaller in the narrow pore and those of the counter-ions are greater in the narrow pore.

Following a step-like rise of the vesicular concentration of K^+ and glutamate$^-$ from 30 to 75 mmol/l the total K^+ and glutamate$^-$ fluxes (these are effluxes because their direction is from the

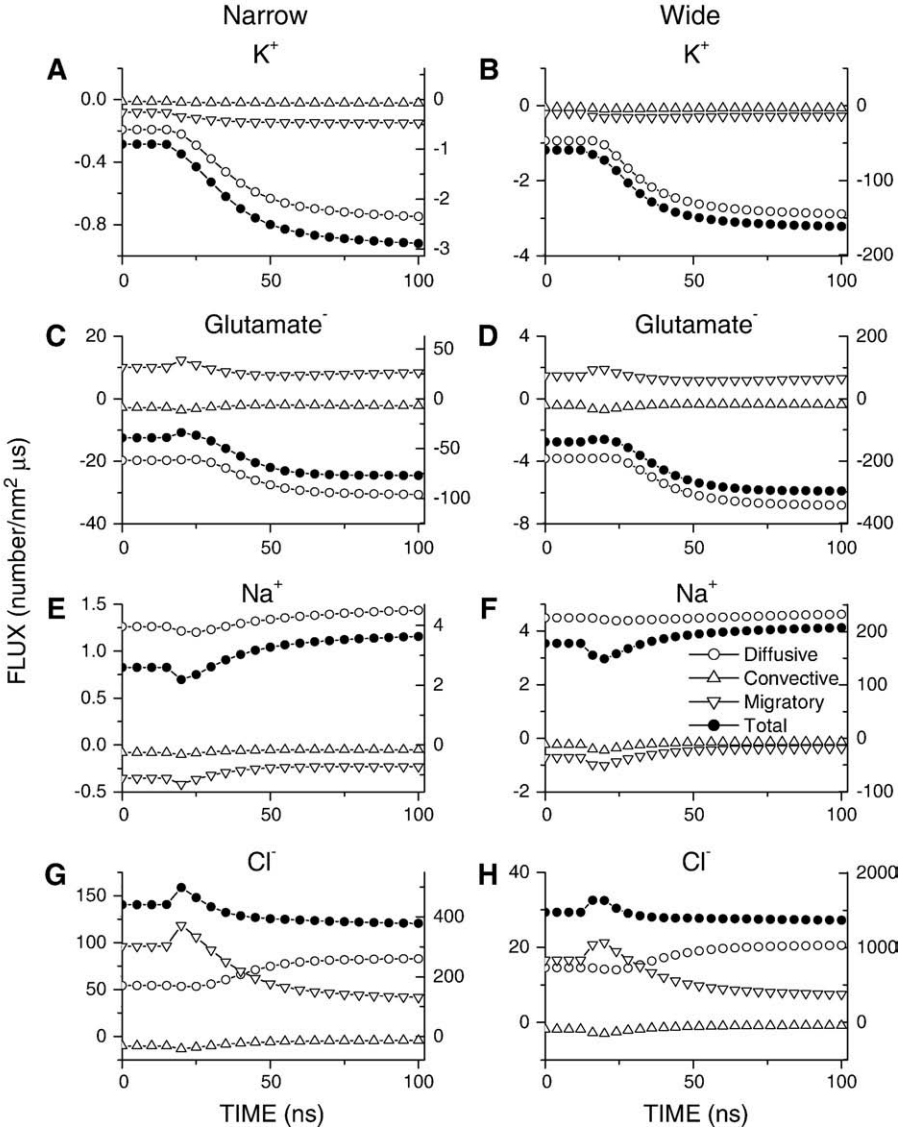

Fig. 10. (A–D) Unitary effluxes of K^+ and glutamate$^-$ become greater as their vesicular concentration rises from 30 to 75 mmol/l, reaching their new steady-state levels in ~50 ns, and are largely diffusive. Migratory flux makes a small contribution rendering the total efflux of K^+ greater and of glutamate$^-$ smaller. In the narrow pore the unitary total efflux of K^+ is smaller, and of glutamate$^-$ much greater than in the wide pore. (E–H) Na^+ and Cl^- fluxes also change but bi-phasically as a result of a rise in the vesicular K^+–glutamate$^-$ concentration, although their extra-cellular concentration does not change. Vesicular pressure was 0 Pa and the potential was 0 mV.

vesicular interior into the extra-cellular space) increase reaching a new steady-state level. The half-times are — 20 ns (K^+; 'narrow pore'), 19 ns (K^+; 'wide pore'), 25 ns (glutamate$^-$; 'narrow pore'), 29 ns (glutamate$^-$; 'wide pore'). Note that whereas the K^+ migratory flux is negative (an efflux) and renders the total K^+ flux larger, the glutamate$^-$ migratory flux is positive (an influx) and renders the total glutamate$^-$ flux smaller. Finally note that the glutamate$^-$ flux is almost thirty times greater than K^+ flux for a narrow pore, but only approximately twice as large than K^+ flux for a wide pore. The flux of co-ions is always smaller than that of counter-ions, but is especially so when the pore is narrow.

It is not surprising that Na^+ and Cl^- ions enter into the pore. The concentration gradient between the extra-cellular and vesicular compartments is large. It is also not surprising that the influx of Cl^- ions is much greater than the influx of Na^+ ions, and that the difference is especially great when the pore is narrow. Cl^- is a counter-ion whereas Na^+ is a co-ion, and the fixed charges on the pore wall influence the concentrations and fluxes more when the pore is narrow. Nevertheless note that Cl^- flux is approximately a hundred times greater than Na^+ flux for the narrow pore but only approximately seven times greater than Na^+ flux for the wide pore. It is however, but only moderately surprising that the influx of Na^+ and Cl^- ions changes when the vesicular K^+–glutamate$^-$ concentration changes, although the extra-cellular concentration of Na^+ and Cl^- ions does not change. The relative changes of both Na^+ and Cl^- fluxes are comparatively small. Their time courses are also bi-phasic, but are completed over a similar time interval as changes of K^+ and glutamate$^-$ fluxes. The half-times are — 34 ns (Na^+; 'narrow pore'), 33 ns (Na^+; 'wide pore'), 34 ns (Cl^-; 'narrow pore'), 33 ns (Cl^-; 'wide pore'). The most likely explanation is that following the rise of the vesicular K^+–glutamate$^-$ concentration the glutamate$^-$ influx into the pore is greater than K^+ influx, because glutamate$^-$ is a counter-ion. To maintain the electrical neutrality of the pore Na^+ influx rises, and Cl^- influx diminishes.

3.7. Step-like change of vesicular K^+–glutamate$^-$ concentration does not alter the force acting on the pore wall

Given that the step-like change of the vesicular K^+–glutamate$^-$ concentration alters not only the concentration (and flux) of ions and glutamate$^-$ but also water velocity and electric potential in the pore it is important to evaluate how such a change alters the radial forces (inertial, viscotic, pressure and electrostatic) acting on the pore wall since these radial forces will influence the pore dilatation and contraction. As Fig. 11A–B shows the total force is affected only marginally (the force becomes more negative and would thus tend to close the pore more) as a result of rise of vesicular K^+–glutamate$^-$ concentration from 30 to 75 mmol/l if the pore is narrow, whereas if the pore is wide the effect is not visible at all (Fig. 11C–D).

4. Discussion

4.1. Simulation of stationary and non-stationary transport through a charged nanosize pore and evaluation of forces acting on pore wall

Glutamate$^-$, K^+, Na^+, Cl^- ion distributions and fluxes as well as potential, water velocity and pressure profiles in charged nanosize pores of different widths were studied using continuum theory. The potential and concentration profiles were calculated using Poisson–Nernst–Planck theories [44,47], which are suitable for evaluation of non-equilibrium problems. Briefly, Nernst–Planck equation combines Ohm's law for the drift of ions in a potential gradient and Fick's law of diffusion due to a concentration gradient. When such a set of equations is combined, it forms a widely used theoretical tool for simulation of many problems in physics, chemistry and biology — Poisson–Nernst–Planck or PNP theory [48,49].

The effect of water flux on the transport of ions is possible to ignore in most ion channels, because of their narrowness and a lack of pressure gradient between the intra- and extra-cellular compartments. However, in the fusion pore this is not possible because of significant vesicular pressure, which in wide pores results in large water velocity, and which in turn leads to significant convective flux of ions and glutamate$^-$ [26]. We thus used a coupled system of Poisson–Nernst–Planck and Navier–Stokes or PNP–NS equations [24,26] to describe the transport of K^+, Na^+, Cl^- ions and glutamate$^-$ and to evaluate the diffusional and kinetic, but also the fluidic factors involved (such as pressure and water velocity) for stationary as well as time-dependent systems. The forces on the pore wall due to these factors were also calculated. The concentration and fluxes (diffusive, migratory and convective) of Na^+, Cl^-, K^+ and glutamate$^-$, fluid (water) velocity and pressure, potential and electric field were calculated throughout a computational domain consisting of a charged nanofluidic pore 10 nm long and whose radius ranged from 1 nm ('narrow' pore) to 4 nm ('wide' pore). The pore was flanked on each side with a compartment representing the vesicular interior and extracellular space [26]. Four forces acting on the wall of the fusion pore were estimated – inertial forces, pressure, viscotic forces, and electrostatic forces – by integrating their values on the boundary 5 (Fig. 1). Integrating inertial, viscous and electrostatic forces amounted to integrating the radial components of their vectors on the boundary. Given that the direction of the force due to the pressure is defined by the surface its radial component at two curved segments at the upper and lower mouth of the pore had first to be calculated and then integrated.

The simulation conditions were as follows (for details see Methods and Results). The surface charge was positive and its density on the membrane facing the pore ranged from $4*10^{-3}$ to $64*10^{-3}$ C/m^2, whereas the density on the membrane facing two compartments was zero. In most simulations there was no pressure or potential difference

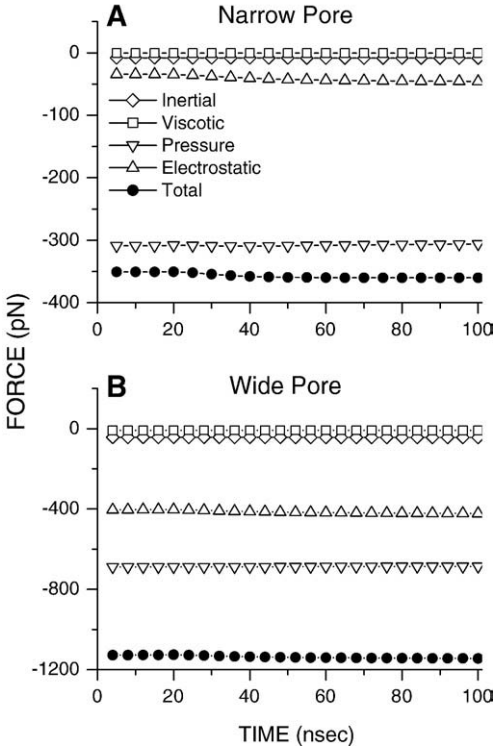

Fig. 11. Total radial force acting on the pore wall and its all four components – inertial, viscotic, pressure and electrostatic force – change only marginally as the vesicular K^+–glutamate$^-$ concentration rises from 30 to 75 mmol/l irrespective of whether the pore is narrow (A) or wide (B). Vesicular pressure was 0 Pa and the potential was 0 mV.

between the control boundaries of the upper (vesicular) and lower (extra-cellular) compartments. In some cases however the pressure difference between two control boundaries (on the upper and lower compartment) ranged from 10^4 to 10^6 Pa, whereas the potential ranged from zero to 100 mV. The K^+–glutamate$^-$ concentration in the upper compartment was 30 mmol/l (stationary simulations), or started from 30 mmol/l but at a chosen time changed in a step-like manner to 75 mmol/l (time-dependent simulations). In the lower compartment it was 0 mM. Na^+–Cl^- concentration was 0 mM/l in the upper compartment and 150 mM in the lower compartment. The following are most important conclusions of this study.

4.2. Electrostatic and pressure forces acting on the pore wall strongly depend on density of pore wall fixed charges but also on pore radius

The viscous and inertial forces acting on the pore wall are as a rule very small, but the electrostatic and pressure forces can be significant. Vesicular pressure determines the pressure-force at the pore wall, if the vesicular pressure is high, and if the charge density on the pore wall is low, irrespective of whether the pore is narrow or wide. The pressure-force is then positive, dominates the total force at the wall and acts to open the pore. The importance of the vesicular pressure, even when it is high, is greatly reduced when the charge density on the pore wall is elevated, because the electro-kinetically induced pressure, which is negative (and thus acting to close the pore) becomes dominant. However, the electro-kinetically induced pressure and pressure-force on the pore wall are influenced, not only by the charge density but also by the pore radius. Both are negative and become more so as the pore dilates. The contribution of the electrostatic force to the total force rises and becomes significant, if the charge density on the pore wall is high and the pore wide. The force is then negative, and thus also tends to close the pore.

Both factors that influence the electrostatic and pressure force (pore radius and charge density) contribute 'directly' but also 'indirectly' to the force on the pore wall. If the surface area increases (owing to pore widening), the pressure force will increase. Greater amount of charge on the pore wall due to the greater surface area leads to greater electrostatic force. The electrostatic force is proportional to the product of the charge and the electric field at the pore wall (see Appendix). However, the amount of charge will also rise if charge density on the pore wall increases. As a result of change of the pore radius and charge density the electrostatic force may also change 'indirectly', because the 'physics' of the situation changes — because the wall pressure and the electric field are altered, and they are. Interestingly, one factor does not alter either the wall pressure or electric field — the vesicular K^+–glutamate$^-$ concentration. It is thus not surprising that the total force in the radial direction is not altered by the addition of a high concentration of Ca^{2+} to the vesicular K^+–glutamate$^-$. This argues that any action that the vesicular Ca^{2+} may have on the extrusion of the vesicular content is not likely to occur by changes of the radial forces acting on the pore wall, and which are generated by the extrusion of the vesicular content.

The influence of the pore wall density of fixed charges on the electric field and pressure at the pore wall is not surprising because: a) the electric field is determined by the presence of the fixed and mobile charges, and b) the pore wall charge density affects the fluxes of ions and glutamate$^-$, influences the electro-kinetically induced pressure and thus pressure on the pore wall. Detailed evaluation revealed that the electric field at the pore wall becomes more negative as the charge density rises, and the relationship is linear going through origin. Nevertheless the electrostatic force depends supra-linearly on the charge density owing to the greater amount of charge on the pore wall. The wall pressure also becomes more negative as the charge density rises. The wall pressure vs. charge density relationship is however, supra-linear, as is the electrostatic force vs. charge density relationship.

Future studies should provide the experimental verification of how the changes in charge density on the pore wall affect pore dynamics. Nevertheless, at the adrenal medullary cells the quantal size (and thus the amount of the transmitter released) was shown to decrease significantly with higher pH [50]. Lower quantal size may be caused by the pH changes in the extra-cellular solution on depolymerization of the vesicular matrix following fusion pore opening [50]. However, such pH changes will also alter the charge density on the wall of the fusion pore, which should subsequently change not only the efflux of the transmitter [26], but as this study suggests the fusion pore dynamics as well.

4.3. Force on pore wall is only marginally affected by potential difference between vesicular and extracellular compartments, by glutamate$^-$ or ion diffusion constants or by water viscosity

Step-like depolarization of the secretory cell leads to a transient but significant rise of the quantal size [7]. The rapid, and spatially highly localized rise of sub-membrane Ca^{2+} [51] may lead to a preferential release of large vesicles, as these are likely to be more effective barriers to Ca^{2+} diffusion [10]. Alternatively membrane depolarization may, through an as yet unknown mechanism facilitate homotypic fusion of secretory granules [52]. However, the step-like depolarization of the secretory cell membrane may also result in the potential change within the vesicle that fused with the plasma membrane, and also in the fusion pore [53]. This in turn could alter the spatial profiles of charged particles, force on the pore wall, fusion pore dynamics and thus the quantal size. We restricted ourselves to evaluating whether the potential difference between the vesicular and extra-cellular compartments affects the forces on the wall of the fusion pore. Even if the potential difference is 100 mV instead of 0 mV the force on the pore wall remains essentially the same, except when the pore is narrow and the density of fixed charges on the pore wall is low, where a small change is visible.

Molecular dynamics simulations have shown that the diffusion of ions and molecules is significantly slower and water viscosity significantly greater in a confined space such as a cylindrical pore and may be further reduced when the pore wall is charged [24,43,46,54]. This study demonstrates however that the force on the pore wall is largely unaffected even by large changes of the diffusion constants of ions (K^+, Na^+ and Cl^-) and glutamate$^-$ or by similarly large changes of water viscosity.

4.4. Step-like change of vesicular K^+ and glutamate$^-$ concentration alters their pore concentration but not space charge density or force on pore wall

The vesicular concentration of transmitter, hormone peptides and ions can change rapidly due to a release through the fusion pore or owing to their dissociation from the gel matrix [55]. It may be argued that such a change will generate significant though transient forces on the pore wall. This study however, reveals that though the concentration of both K^+ and glutamate$^-$ in the fusion pore rises very rapidly as a result of a step-like rise of vesicular K^+–glutamate$^-$ concentration the space charge density does not change or only marginally (the mean value or spatial distribution). It is thus not surprising that the electrostatic force on the pore wall remains the same. Interestingly, the pressure and the force due to the pressure acting on the pore wall also remain essentially constant. Since the viscotic and inertial forces are as a rule very small, the total force acting on the pore wall remains unaffected.

Nevertheless the chain of events in the fusion pore initiated by a step-like increase of the vesicular concentration of K^+–glutamate$^-$ concentration is not negligible and their evaluation provides interesting insights. Greater concentration of K^+ and glutamate$^-$ in the

vesicle results in their greater entry into the pore and in their greater efflux. Both changes are essentially completed in <100 ns. These changes are also associated with changes of the Na^+ and Cl^- concentration in the pore (similarly completed in <100 ns), although their extra-cellular concentration remained constant. Na^+ and Cl^- concentration changes are probably due to the electrostatic (but also electrokinetic and fluidic) forces, which strongly favor the maintenance of the approximate electrical neutrality of the pore. They are however in good agreement with a recent report suggesting that the transmitter release is not associated with cation flux through channels in the vesicle membrane, but with Na^+ influx through the fusion pore [56]. Finally, given that the fluxes of charged particles (ions and glutamate$^-$) were altered, it is not surprising that the water velocity changed too, although the time course of its change is more complicated. It first rises before diminishing to a lower steady-state level, but the change is completed within a similar short time interval (<100 ns).

4.5. Force generated by the extrusion of vesicular content can be sufficiently large to overcome forces caused by the tension difference between vesicular and plasma membrane

Finally the question arises whether the forces on the fusion pore wall generated by the extrusion of vesicular content are sufficiently large to overcome forces in the membrane caused by the tension difference between vesicular and plasma membrane [57]. Comparison of these forces shows that they are of similar order. Moreover, whereas the forces in the membrane remain essentially constant, those acting on the pore wall increase steeply as the pore dilates [58]. Moreover, the forces in the membrane are likely to diminish during dilatation, because the tension difference will probably not be maintained. Therefore as the pore dilates owing to the forces in the membrane, the extrusion of the vesicular content simultaneously generates forces in the pore, which increase and may become stronger to initiate closure of the fusion pore. It is still to be determined whether this is the main or one of several mechanisms determining whether the release of the vesicular content will be an all-or-none or a kiss-and-run event.

5. Conclusion

In conclusion we simulate a combined diffusion/migration/convection flow of glutamate$^-$ K^+, Na^+ and Cl^- ions and water through charged nano-pore using continuum theory. We estimate the forces acting on the pore wall generated by such flows. Four forces are considered — inertial, viscotic, pressure and electrostatic. Whereas the inertial and viscotic forces are typically small the pressure and electrostatic force are significant and if the charge density on the pore wall is not low the direction of both forces is to close the fusion pore. The extrusion of glutamate$^-$, ions and water by itself generates the forces to close the fusion pore.

Acknowledgments

Support by the grants from the Heart and Stroke Foundation of Canada, National Science and Engineering Council of Canada and Canadian Institutes of Health Research to M.I.G. is acknowledged.

Appendix

Calculation of forces acting on fusion pore wall

The forces acting on the wall of the fusion pore were calculated as follows. Given the axial symmetry in z-direction used in these simulations, all variables (e.g. fluid velocity, electrical field) in θ direction are ignored. In 2D r–z plane of the cylindrical coordinate system the simplified Navier–Stokes equation expressed in terms of the components of the stress tensor τ becomes:

r−component

$$:\rho\left(\frac{\partial u}{\partial t}+u\frac{\partial u}{\partial r}+v\frac{\partial u}{\partial z}\right)=-\frac{\partial p}{\partial r}-\left[\frac{1}{r}\frac{\partial}{\partial r}(r\tau_{rr})+\frac{\partial \tau_{rz}}{\partial z}\right]+F_{e-r} \tag{8}$$

z−component

$$:\rho\left(\frac{\partial v}{\partial t}+u\frac{\partial v}{\partial r}+v\frac{\partial v}{\partial z}\right)=-\frac{\partial p}{\partial z}-\left[\frac{1}{r}\frac{\partial}{\partial r}(r\tau_{rz})+\frac{\partial \tau_{zz}}{\partial z}\right]+F_{e-z} \tag{9}$$

where u and v are the r- and z-components of the fluid velocity, respectively.

For a Newtonian fluid in 2D r–z plane (of the cylindrical coordinate system) the ij-th components, τ_{ij}, of the viscous stress tensor τ, are defined as:

$$\tau_{rr}=-\mu\left[2\frac{\partial u}{\partial r}-\frac{2}{3}(\nabla.\mathbf{u})\right] \tag{10}$$

$$\tau_{zz}=-\mu\left[2\frac{\partial v}{\partial z}-\frac{2}{3}(\nabla.\mathbf{u})\right] \tag{11}$$

$$\tau_{rz}=-\mu\left[\frac{\partial v}{\partial r}+\frac{\partial u}{\partial z}\right] \tag{12}$$

where

$$\nabla.\mathbf{u}=\frac{1}{r}\frac{\partial}{\partial r}(ru)+\frac{\partial v}{\partial z}. \tag{13}$$

Finally, $\mathbf{F}_e=\rho_c\nabla\Phi$, where the gradient operator in the cylindrical coordinate system is given by:

$$[\nabla\Phi]_r=\frac{\partial\Phi}{\partial r},[\nabla\Phi]_z=\frac{\partial\Phi}{\partial z}. \tag{14}$$

If we substitute the components of the stress tensor (Eqs. 10–13), into the Eqs. (8) and (9), we obtain Eqs. (15) and (16) describing the Navier–Stokes equation in terms of velocity gradients, but in a computationally friendly form. They are as follows:

r−component

$$:\rho\left(\frac{\partial u}{\partial t}+u\frac{\partial u}{\partial r}+v\frac{\partial u}{\partial z}\right)=-\frac{\partial p}{\partial r}+\mu\left[\frac{\partial}{\partial r}\left(\frac{1}{r}\frac{\partial}{\partial r}(ru)\right)+\frac{\partial^2 u}{\partial z^2}\right]+\rho_e\frac{\partial\Phi}{\partial r} \tag{15}$$

z−component

$$:\rho\left(\frac{\partial v}{\partial t}+u\frac{\partial v}{\partial r}+v\frac{\partial v}{\partial z}\right)=-\frac{\partial p}{\partial z}+\mu\left[\frac{1}{r}\frac{\partial}{\partial r}\left(r\frac{\partial v}{\partial r}\right)+\frac{\partial^2 v}{\partial z^2}\right]+\rho_e\frac{\partial\Phi}{\partial z}. \tag{16}$$

The total stress tensor ($\mathbf{T}$), comprises of pressure and viscous stress tensor (and which is needed to calculate the total force acting on the surfaces of the pore) as follows:

$$\mathbf{T}=-p\mathbf{I}+\boldsymbol{\tau} \tag{17}$$

where $\mathbf{I}$ is the unity tensor. Finally, the total force acting on the pore surface is calculated as:

$$F_i=\oint T_{ij}\mathrm{d}S_j+F_{e-i} \tag{18}$$

where the component T_{ij} of the total stress tensor is the i-th component of the fluidic force applied to a unit area perpendicular to the x_j axis.

References

[1] L.J. Breckenridge, W. Almers, Currents through the fusion pore that forms during exocytosis of a secretory vesicle, Nature 328 (1987) 814–817.
[2] L.J. Breckenridge, W. Almers, Final steps in exocytosis observed in a cell with giant secretory granules, Proc. Natl. Acad. Sci. U. S. A. 84 (1987) 1945–1949.
[3] D. Sulzer, E.N. Pothos, Regulation of quantal size by presynaptic mechanisms, Rev. Neurosci. 11 (2000) 159–212.
[4] C. Pawlu, A. DiAntonio, M. Heckmann, Postfusional control of quantal current shape, Neuron 42 (2004) 607–618.
[5] X. Wang, K.L. Engisch, R.W. Teichert, B.M. Olivera, M.J. Pinter, M.M. Rich, Activity-dependent presynaptic regulation of quantal size at the mammalian neuromuscular junction in vivo, J. Neurosci. 25 (2005) 343–351.
[6] J.C. Behrends, G. ten Bruggencate, Changes in quantal size distributions upon experimental variations in the probability of release at striatal inhibitory synapses, J. Neurophysiol. 79 (1998) 2999–3011.
[7] M.I. Glavinović, J.M. Trifaro, Change of quantal size and parameters of release with stimulation in bovine chromaffin cells, Pflügers Arch. 443 (2002) 584–592.
[8] Z. Chiti, A.G. Teschemacher, Exocytosis of norepinephrine at axon varicosities and neuronal cell bodies in the rat brain, FASEB J. 21 (2007) 2540–2550.
[9] A.J. Cochilla, J.K. Angleson, W.J. Betz, Differential regulation of granule-to-granule granule-to plasma membrane fusion during secretion from rat pituitary lactotrophs, J. Cell Biol. 150 (2000) 839–848.
[10] M.I. Glavinović, H.R. Rabie, Monte Carlo evaluation of quantal analysis in the light of Ca^{2+} dynamics the geometry of secretion, Pflugers Arch. 443 (2001) 132–145.
[11] B. Ceccarelli, W.P. Hurlbut, A. Mauro, Turnover of transmitter synaptic vesicles at the frog neuromuscular junction, J. Cell Biol. 57 (1973) 499–524.
[12] A.M. Aravanis, J.L. Pyle, R.W. Tsien, Single synaptic vesicles fusing transiently successively without loss of identity, Nature 423 (2003) 643–647.
[13] D.A. Richards, J. Bai, E.R. Chapman, Two modes of exocytosis at hippocampal synapses revealed by rate of FM1-43 efflux from individual vesicles, J. Cell Biol. 168 (2005) 929–939.
[14] B. Granseth, B. Odermatt, S.J. Royle, L. Lagnado, Clathrin-mediated endocytosis is the dominant mechanism of vesicle retrieval at hippocampal synapses, Neuron 51 (2006) 773–786.
[15] S. Choi, J. Klingauf, R.W. Tsien, Postfusional regulation of cleft glutamate concentration during LTP at 'silent synapses', Nature Neurosci. 3 (2000) 330–336.
[16] P. Neco, C. Fernández-Peruchena, S. Navas, L.M. Gutiérrez, G. Alvarez de Toledo, E. Alés, Myosin II contributes to fusion pore expansion during exocytosis, J. Biol. Chem. 283 (2008) 10949–10957.
[17] T.R. Cheek, R.D. Burgoyne, Cyclic AMP inhibits both nicotine-induced actin disassembly catecholamine secretion from bovine adrenal chromaffin cells, FEBS Lett. 207 (1986) 110–114.
[18] M.L. Vitale, E.P. Seward, J.M. Trifaro, Chromaffin cell cortical actin network dynamics control the size of the release-ready vesicle pool and the initial rate of exocytosis, Neuron 14 (1995) 353–363.
[19] M. Oheim, D. Loerke, W. Stuhmer, R.H. Chow, Multiple stimulation-dependent processes regulate the size of the releasable pool of vesicles, Eur. Biophys. J. 28 (1999) 91–101.
[20] P. Neco, D. Giner, S. Viniegra, R. Borges, A. Villarroel, L.M. Gutiérrez, New roles of myosin II during vesicle transport and fusion in chromaffin cells, J. Biol. Chem. 279 (2004) 27450–27457.
[21] O. Söderman, B. Jönsson, Electro-osmosis: velocity profiles in different geometries with both temporal and spatial resolution, J. Chem. Phys. 105 (1996) 10300–10311.
[22] N.A. Patankar, H.H. Hu, Numerical simulation of electroosmotic flow, Anal. Chem. 70 (1998) 1870–1881.
[23] P. Dutta, A. Beskok, Analytical solution of combined electroosmotic/pressure driven flows in two-dimensional straight channels: finite Debye layer effects, Anal. Chem. 73 (2001) 1979–1986.
[24] R. Qiao, N.R. Aluru, Ion concentrations velocity profiles in nanochannel osmotic flows, J. Chem. Phys. 118 (2003) 692–4701.
[25] H. Daiguji, P. Yang, A. Majumdar, Ion transport in nanofluidic channels, Nano Lett. 4 (2004) 137–142.
[26] G. De Luca, M.I. Glavinović, Glutamate, water and ion transport through a charged nanosize pore, Biochim. Biophys. Acta – Biomemb. 1768 (2007) 264–279.
[27] S.G.A. McLaughlin, G. Szabo, G. Eisenman, Divalent ions and the surface potential of charged phospholipid membranes, J. Gen. Physiol. 58 (1971) 667–687.
[28] B. Hille, A.M. Woodhull, B.I. Shapiro, Negative surface charge near sodium channels of nerve: divalent ions, monovalent ions, and pH, Phil. Trans. R. Soc. Lond. B Biol. Sci. 270 (1975) 301–318.
[29] J. Barthel, H. Krienke, W. Kunz, Physical Chemistry of Electrolyte Solutions: Modern Aspects, Springer, New York, 1998.
[30] S. Durand-Vidal, J.-P. Simonin, P. Turq, Electrolytes at Interfaces, Kluwer, Boston, 2000.
[31] S.W. Chiu, J.A. Novotny, E. Jakobsson, The nature of ion and water barrier crossings in a simulated ion channel, Biophys. J. 64 (1993) 96–108.
[32] B.P. Jena, S.J. Cho, A. Jeremic, M.H. Stromer, R. Abu-Hamdah, Structure and composition of the fusion pore, Biophys. J. 84 (2003) 1337–1343.
[33] X. Han, M.B. Jackson, Structural transitions in the synaptic SNARE complex during Ca2+-triggered exocytosis, J. Cell Biol. 172 (2006) 281–293.
[34] P.R. Maycox, T. Deckwerth, J.W. Hell, R. Jahn, Glutamate uptake by brain synaptic vesicles. Energy dependence of transport and functional reconstitution in proteoliposomes, J. Biol. Chem. 263 (1988) 15423–15428.
[35] H.B. Pollard, H. Shindo, C.E. Creutz, C.J. Pazoles, J.S. Cohen, Internal pH and state of ATP in adrenergic chromaffin granules determined by 31P nuclear magnetic resonance spectroscopy, J. Biol. Chem. 254 (1979) 1170–1177.
[36] D. Njus, P.M. Kelley, G.J. Harnadek, Bioenergetics of secretory vesicles, Biochim. Biophys. Acta 853 (1986) 237–265.
[37] R.G. Johnson, Accumulation of biological amines into chromaffin granules: a model for hormone and neurotransmitter transport, Physiol. Rev. 68 (1988) 232–307.
[38] E.N. Pothos, E. Mosharov, K.P. Liu, W. Setlik, M. Haburcak, G. Baldini, M.D. Gershon, H. Tamir, D. Sulzer, Stimulation-dependent regulation of the pH, volume and quantal size of bovine and rodent secretory vesicles, J. Physiol. 542 (2002) 453–476.
[39] P.P. Atluri, T.A. Ryan, The kinetics of synaptic vesicle reacidification at hippocampal nerve terminals, J. Neurosci. 26 (2006) 2313–2320.
[40] A.L. Lehninger, Biochemistry, Worth Publishers Inc., New York, 1970.
[41] G. Hummer, J.C. Rasaiah, J.P. Noworyta, Water conduction through the hydrophobic channel of a carbon nanotube, Nature 414 (2001) 188–190.
[42] R. Qiao, N.R. Aluru, Atypical dependence of electroosmotic transport on surface charge in a single-wall carbon nanotube, Nano Lett. 3 (2003) 1013–1017.
[43] S.M. Cory, Y. Liu, M.I. Glavinović, Interfacial interactions of glutamate, water ions with carbon nanopore evaluated by molecular dynamics simulations, Biochim. Biophys. Acta – Biomemb. 1768 (2007) 2319–2341.
[44] B. Corry, S. Kuyucak, S.H. Chung, Tests of continuum theories as models of ion channels. II. Poisson Nernst Planck Theory versus Brownian dynamics, Biophys. J. 78 (2000) 2364–2381.
[45] M.L. Mundorf, K.P. Troyer, S.E. Hochstetler, J.A. Near, R.M. Wightman, Vesicular Ca (2+) participates in the catalysis of exocytosis, J. Biol. Chem. 275 (2000) 9136–9142.
[46] G.R. Smith, M.S.P. Sansom, Effective diffusion coefficients of K^+ and Cl^- ions in ion channel models, Biophys. Chem. 79 (1999) 129–151.
[47] G. Moy, B. Corry, S. Kuyucak, S.H. Chung, Tests of continuum theories as models of ion channels. I. Poisson–Boltzmann theory versus Brownian dynamics, Biophys. J. 78 (2000) 2349–2363.
[48] J.O.M. Bockris, A.K.N. Reddy, Modern Electrochemistry, Plenum Publ., New York, 1976.
[49] J.S. Newman, Electrochemical Systems, 2nd ed.Prentice Hall, Englewood Cliffs, NJ, 1991.
[50] J.A. Jankowski, T.J. Schroeder, E.L. Ciolkowski, R.M. Wightman, Temporal characteristics of quantal secretion of catecholamines from adrenal medullary cells, J. Biol. Chem. 268 (1993) 14694–14700.
[51] S.M. Simon, R.R. Llinas, Compartmentalization of the submembrane activity during calcium influx and its significance in transmitter release, Biophys. J. 48 (1985) 485–498.
[52] S. Urbe, L.J. Page, S.A. Tooze, Homotypic fusion of immature secretory granules during maturation in a cell-free assay, J. Cell Biol. 143 (1998) 1831–1844.
[53] C. Nanavati, J.M. Fernandez, The secretory granule matrix: a fast acting smart polymer, Science 259 (1993) 963–965.
[54] S. Joseph, N.R. Aluru, Why are carbon nanotubes fast transporters of water? Nano Lett. 8 (2008) 452–458.
[55] H.R. Rabie, J. Rong, M.I. Glavinović, Monte Carlo simulation of release of vesicular content in neuroendocrine cells, Biol. Cybern. 94 (2006) 483–499.
[56] L.W. Gong, G. Alvarez de Toledo, M. Lindau, Exocytotic catecholamine release is not associated with cation flux through channels in the vesicle membrane but Na+ influx through the fusion pore, Nat. Cell Biol. 9 (2007) 915–922.
[57] Y.A. Chizmadzhev, D.A. Kumenko, P.I. Kuzmin, L.V. Chernomordik, J. Zimmerberg, F. Cohen, Lipid flow through fusion pores connecting membranes of different tensions, Biophys. J. 76 (1999) 2951–2965.
[58] M. Tajparast, M.I. Glavinović, Forces and stresses acting on fusion pore membrane during secretion, Biophys. J. (2009), doi:10.1016/j.bbamem.2009.01.019.